



**Fermi National Accelerator Laboratory**

**FERMILAB-Pub-97/402**

**Calibrating the Energy of a 50 x 50 GeV Muon Collider  
Using Spin Precession**

Rajendran Raja and Alvin Tollestrup

*Fermi National Accelerator Laboratory  
P.O. Box 500, Batavia, Illinois 60510*

December 1997

Submitted to *Physical Review D*

## **Disclaimer**

*This report was prepared as an account of work sponsored by an agency of the United States Government. Neither the United States Government nor any agency thereof, nor any of their employees, makes any warranty, expressed or implied, or assumes any legal liability or responsibility for the accuracy, completeness, or usefulness of any information, apparatus, product, or process disclosed, or represents that its use would not infringe privately owned rights. Reference herein to any specific commercial product, process, or service by trade name, trademark, manufacturer, or otherwise, does not necessarily constitute or imply its endorsement, recommendation, or favoring by the United States Government or any agency thereof. The views and opinions of authors expressed herein do not necessarily state or reflect those of the United States Government or any agency thereof.*

## **Distribution**

*Approved for public release; further dissemination unlimited.*

**Calibrating the energy of a  $50 \times 50$  GeV muon collider using spin  
precession**

Rajendran Raja

&

Alvin Tollestrup

*Fermi National Accelerator Laboratory*

*P.O. Box 500*

*Batavia, IL 60510*

**Abstract**

The neutral Higgs boson is expected to have a mass in the region 90-150 GeV/c<sup>2</sup> in various schemes within the Minimal Supersymmetric extension to the Standard Model. A first generation Muon Collider is uniquely suited to investigate the mass, width and decay modes of the Higgs boson, since the coupling of the Higgs to muons is expected to be strong enough for it to be produced in the  $s$  channel mode in the muon collider. Due to the narrow width of the Higgs, it is necessary to measure and control the energy of the individual muon bunches to a precision of a few parts in a million. We investigate the feasibility of determining the energy scale of a muon collider ring with circulating muon beams of 50 GeV energy by measuring the turn by turn variation of the energy deposited by electrons produced by the decay of the muons. This variation is caused by the existence of an average initial polarization of the muon beam and a non-zero value of  $g-2$  for the muon. We demonstrate that it is feasible to determine the energy scale of the machine

with this method to a few parts per million using data collected during 1000 turns.

## I. THE METHOD

The spin vector  $\vec{S}$  of a muon in the muon collider will precess according to the following equation, first derived by Bargmann, Michel and Telegdi [1]

$$\frac{d\vec{S}}{dt} = \vec{\Omega} \times \vec{S} \quad (1.1)$$

$$\vec{\Omega} = -\frac{e}{\gamma m_\mu} \left( (1 + a\gamma)\vec{B}_\perp + (1 + a)\vec{B}_\parallel - (a\gamma + \frac{\gamma}{1 + \gamma})\vec{\beta} \times \frac{\vec{E}}{c} \right) \quad (1.2)$$

where  $\vec{B}_\perp$  and  $\vec{B}_\parallel$  are the transverse and parallel components of the magnetic field with respect to the muon's velocity  $\vec{\beta}c$ ,  $e$  is the electric charge,  $m_\mu$  the mass of the muon,  $a \equiv \frac{g-2}{2}$  is the magnetic moment anomaly of the muon and  $\gamma$  and  $g$  are the Lorentz factor and the gyromagnetic ratio of the muon. The value of  $a \equiv \frac{g-2}{2}$  for the muon is 1.165924E-3 [2]. In what follows, we will consider the ideal planar collider ring case where  $\vec{B}_\parallel$  and  $\vec{E}$  are zero. For such a collider ring,  $\vec{\Omega}$  is given by

$$\vec{\Omega} = \vec{\Omega}_{cyc}(1 + a\gamma) \quad (1.3)$$

where  $\vec{\Omega}_{cyc}$  is the angular velocity of the circulating beam. From this, it follows that when the beam completes one turn, the spin will rotate by a further  $a\gamma \times 2\pi$  radians. We will compute the precision with which  $\gamma$  can be determined by measuring the energy of the electrons produced by muon decay in this ideal case. We will examine the effects of departures from the ideal case in the last section.

It can be shown that the angular distribution of the decay electrons in the muon center of mass is given by the relation [3]

$$\frac{d^2N}{dx d\cos\theta} = N(x^2(3 - 2x) - \hat{P}x^2(1 - 2x)\cos\theta) \quad (1.4)$$

where  $N$  denotes the number of muon decays,  $x \equiv 2E/m_\mu$  is the electron energy  $E$  in the muon rest frame expressed as a fraction of the maximum possible energy ( $\approx 0.5m_\mu$ ),  $\cos\theta$  is the angle of the electron in the muon rest frame with respect to the  $z$  axis which is the direction of motion of the muon in the laboratory and  $\hat{P}$  is the product of the muon charge and the  $z$  component of the muon polarization. The muon polarization is defined as the average of the individual muon unit spin vectors over the ensemble of muons considered. We note that the distribution is linear in  $\hat{P}$ .

A routine was written to generate muon decays according to equation 1.4. Figure 1 shows the shape of the function in equation 1.4 and the generated events in  $x, \cos\theta$  space for various values of  $\hat{P}$ . There is excellent agreement between the theoretical shape of the function and the Monte Carlo generated events. The average energy  $\langle E \rangle$  and longitudinal momentum  $\langle P_L \rangle$  of the electron in the muon rest frame can be obtained using equation 1.4 as follows.

$$\langle E \rangle = \frac{m_\mu}{2} \int \int x \frac{d^2 N}{dx d\cos\theta} dx d\cos\theta = \frac{7}{10} \frac{m_\mu}{2} \quad (1.5)$$

$$\langle P_L \rangle = \frac{m_\mu}{2} \int \int x \cos\theta \frac{d^2 N}{dx d\cos\theta} dx d\cos\theta = \frac{\hat{P}}{10} \frac{m_\mu}{2} \quad (1.6)$$

These two quantities form the components of a 4-vector, whose transverse components are zero, which may be transformed to the laboratory frame to yield the average electron energy  $\langle E_{lab} \rangle$ .

$$\langle E_{lab} \rangle = \frac{7}{20} E_\mu \left(1 + \frac{\beta}{7} \hat{P}\right) \quad (1.7)$$

where  $E_\mu$  is the energy of the muon beam. Since the polarization  $\hat{P}$  precesses from turn to turn by the amount  $\omega = \gamma(g-2)/2 \times 2\pi$  radians, and the number of muons decrease turn by turn due to decay and losses, the total energy  $E(t)$  due to decay electrons observed during turn  $t$  in an electromagnetic calorimeter will have the following expression

$$E(t) = N e^{(-\alpha t)} \left( \frac{7}{20} E_\mu \left(1 + \frac{\beta}{7} (\hat{P} \cos\omega t + \phi)\right) \right) \quad (1.8)$$

where  $N$  is the number of muon decays sampled in turn 0,  $\phi$  is an arbitrary phase containing information on the initial direction of polarization and  $\alpha$  is the turn by turn decay constant of the muon intensity which in the absence of losses other than decay is given by

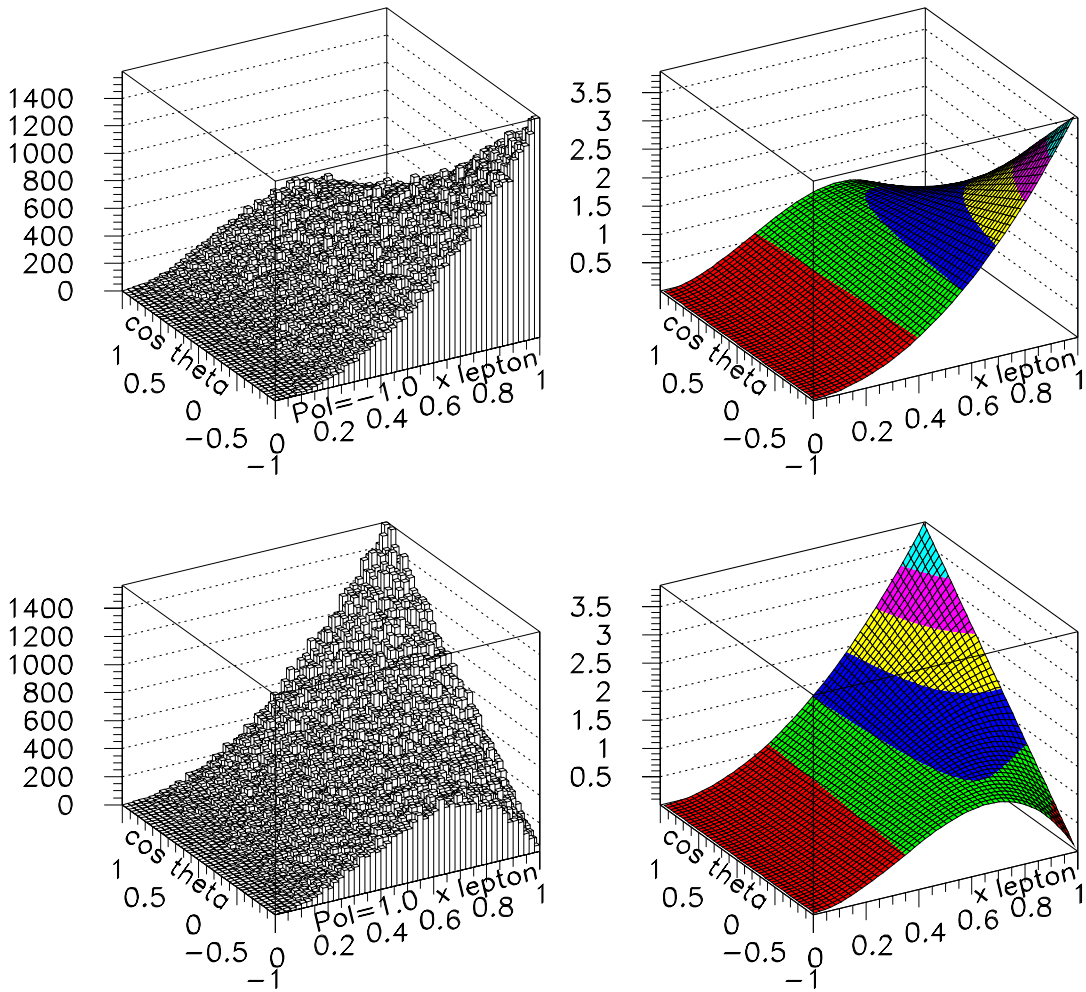


FIG. 1. The top lego plots shows the generated events and the theoretical decay function in the  $x, \cos\theta$  plane for  $\hat{P} = -1.0$ . The lego plots at the bottom of the figure show the corresponding plots for  $\hat{P} = 1.0$ .

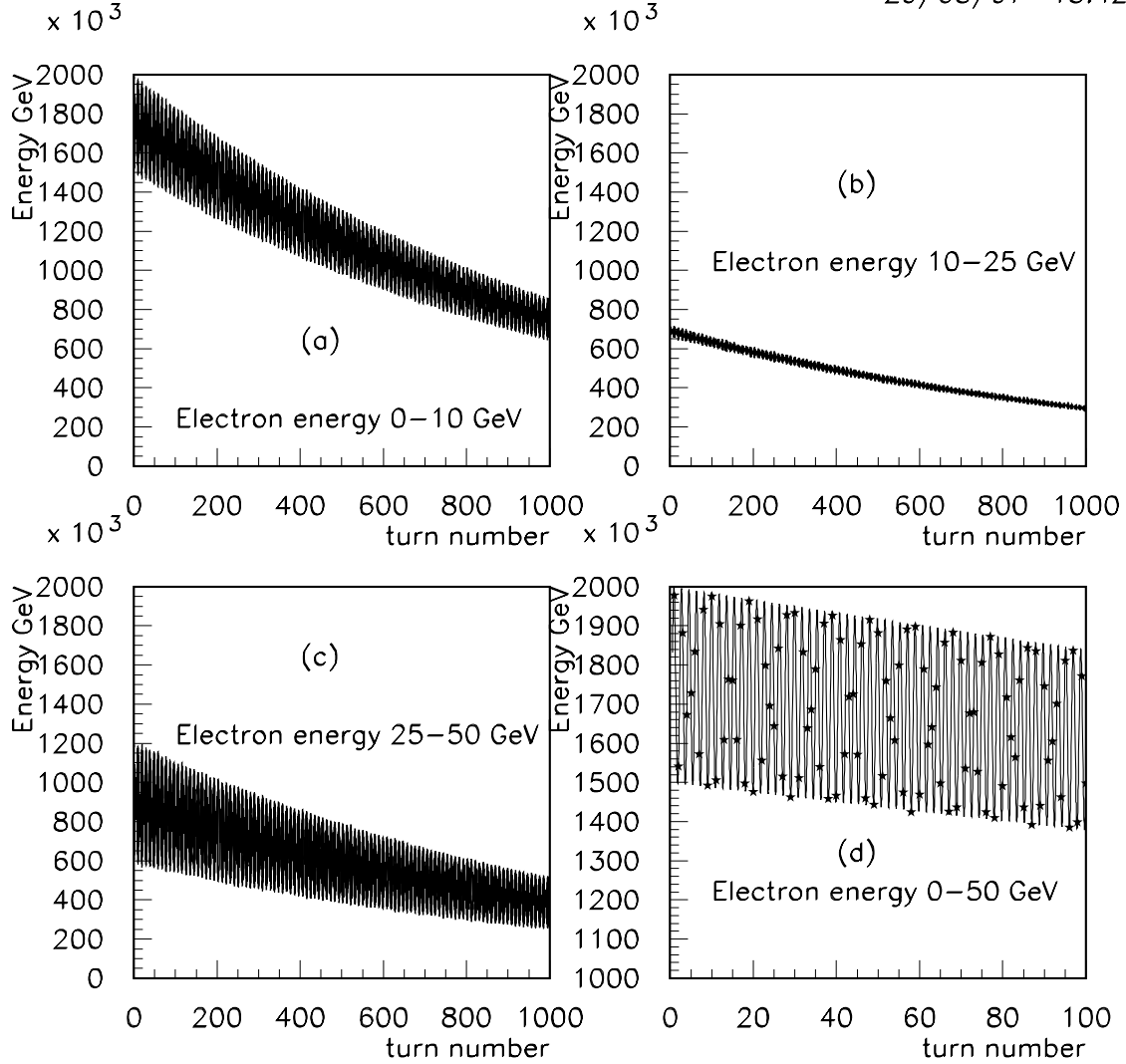


FIG. 2. (a) Total energy observed as a function of turn number for  $\hat{P} = -1.0$  with individual electron energies in the range 0–10 GeV for 100,000 muon decays. (b) Electron energies in the range 10–25 GeV (c) 25–50 GeV (d) All electrons included. Superimposed is a functional form defined by equation 1.8

$$\alpha = \frac{t_{circ}}{\gamma t_{life}} \quad (1.9)$$

where  $t_{circ}$  is the time taken to circulate around the storage ring and  $t_{life}$  is the muon life time.

For a 100% polarized beam, the amplitude of the oscillations is only 1/7 that of the non-oscillating background. It can be seen from equation 1.4 that the sensitivity to  $\hat{P}$  is enhanced by selecting larger values of  $\cos\theta$ . This implies selecting electrons with higher laboratory energy. Figures 2(a-c) show the deposited electron energy as a function of turn number for polarization  $\hat{P} = 1.0$  for individual electron energy ranges of 0-10 GeV, 10-25 GeV and 25-50 GeV respectively as a function of turn number. Figure 2(b) shows very little oscillatory signal, since the electrons in that energy range have small values of  $\cos\theta$ . Figure 2(d) shows the deposited electron energy with no electron energy cuts. Superimposed is the predicted behavior according equation 1.8. This serves as a consistency check for our routines. The signal to background ratio increases as we demand electrons with higher value of  $\cos\theta$ . In what follows, we use electrons with energy greater than 25 GeV during the investigative phase of this analysis and will later optimize this cut. In practice, we can select electrons with energies above a value by momentum analyzing them with a dipole field before they enter the calorimeter.

The method to determine the energy scale of the collider would then entail fitting a functional form of the type

$$f(t) = Ae^{-Bt}(C\cos(D + Et) + F) \quad (1.10)$$

to the energy observed in the calorimeter. The variables  $A, B, C, D, E, F$  are parameters to be fitted. The information on the energy scale is contained in the parameter  $E$ .

### A. Parameters of a 50 GeV idealized muon storage ring

In order to arrive at reasonable numbers for  $\alpha$  and  $\omega$ , we consider a storage ring of 50 GeV muons with a uniform bending field of 4 Tesla. This would produce a circular ring

Parameter	Value	Parameter	Value
Muon Energy	50 GeV	$\gamma$	473.22
spin precession in one turn	3.4667 radians	Magnetic field	4.0 Tesla
radius of ring	41.66666 meters	beam circulation time	0.87327E-06 sec
dilated muon life time	0.10397E-02 sec	turn by turn decay constant	0.8399E-03

TABLE I. Parameters of an idealized muon storage ring

with the parameters given in table I. It should be noted that for an idealized storage ring with constant B field considered here,  $\alpha$  does not depend on  $\gamma$ , since

$$t_{circ} = \frac{m_{\mu}\gamma}{0.3Bc} \quad (1.11)$$

$$\alpha = \frac{2\pi m_{\mu}}{0.3Bct_{life}} \quad (1.12)$$

where  $m_{\mu}$  is the muon rest mass, B is the bending field of the storage ring and  $c$  is the velocity of light. A 100 GeV collider ring will have the same  $\alpha$  as a 50 GeV collider ring or a 25 GeV collider ring in this idealized case. As  $\gamma$  changes slightly,  $t_{circ}$  changes in proportion,  $\alpha$  being the constant used to convert measurements of  $t_{circ}$  to  $\gamma$ . Measuring the decay rate of muons also affords a second method to determine  $\gamma$ . The beam circulation time  $t_{circ}$  can be measured to precisions of the order of a part in  $10^6$  and the fractional error in muon lifetime is 1.82E-5 [2]. The fractional error in  $\gamma$  obtainable by observing the rate of decay of the muons will then be dominated by the precision that one can measure  $\alpha$ , namely  $\delta\gamma/\gamma = \delta\alpha/\alpha$ .

### B. Generation of events and fitting for $\gamma$

Since equation 1.4 is linear in  $\hat{P}$ , the decay distribution of an ensemble of muons depends only on  $\hat{P}$ , the ensemble average of the  $z$  component of the individual muon spin vectors. However, because of the momentum spread of the muons, each individual particle will have

a  $\gamma$  slightly different from the average and hence the precession of the spin vector around the ring will be different, leading to a slightly different value of  $\hat{P}$  for the next turn. We model the beam by generating an ensemble of 100,000 muons each having its own spin vector and momentum. In an actual collider, it will be possible to sample significantly more decays than this. During each turn, we decay all the beam particles once and record the number and total energy deposited by electrons with individual energies above 25 GeV. Approximately 27% of the decay electrons pass this cut, on average. We decrease the number of decays by the appropriate number expected by muon decay alone for the next turn. At this stage we do not introduce fluctuations in the number of decays from turn to turn, since the 100,000 muons are meant to be representative of a much larger number in the actual ring. We process the 100,000 spin vectors by their individual precession rates and make them decay again. We repeat this for 1000 turns. We re-use the muons after each turn since the 100,000 muons represent our model of the muon ensemble in the collider.

### *1. Generation of muon spin vectors*

We generate 4 different samples of events with different ensembles of spin vectors. The  $z$  component of the unit spin vector of a muon  $S_z$  is allowed to vary from -1 to 1. This range is divided into 51 bins and the  $z$  components are generated using a binomial distribution whose average value is specified. We are justified in treating this problem in this classical fashion, since each “muon” represents an ensemble of actual muons with quantized spin components. A more realistic generation of the spin vectors with correlations between momentum spread and  $\hat{P}$  would require a detailed modelling of the pion decay and muon transport systems and is not warranted here since the effect due to the distribution in  $S_z$  is expected to be small. Figures 3 (a-d) show the distributions of  $S_z$  for the 4 samples. The average value of the distributions are 0.9, 0.74, 0.5 and 0.26 respectively. We study negatively charged muons resulting an initial value of  $\hat{P}$  of -0.9,-0.74,-0.5 and -0.26 respectively for these samples. In the absence of momentum spread, the decay distributions would only depend on  $\hat{P}$  and not

on the details of the distribution of  $S_z$ . The angles of the spin vectors are precessed by the individual  $\gamma$  dependent precession rate from turn to turn. In what follows, we assume a beam energy spread of 0.03% for the muons for all samples unless otherwise specified.

## 2. Fitting procedure and generation of errors

The energy deposited every turn is fitted to the functional form given by equation 1.10 using the CERN program MINUIT [4]. In order to study the variation of the fractional error  $\delta\gamma/\gamma$  with the number of electrons sampled, we fluctuate the energy observed in the calorimeter  $E_m$  by

$$\frac{\sigma_{E_m}^2}{\langle E_m \rangle^2} \approx \frac{1}{N}(1.03153) \quad (1.13)$$

where  $N$  is the number of electrons sampled. See Appendix for a derivation of this formula. We analyze the case for 41261, 10315, 2579 and 1146 electrons sampled which corresponds to a fractional error in the measured total energy of  $\text{PERR} \equiv \frac{\sigma_{E_m}}{E_m}$  of .5E-2, 1.0E-2, 2.0E-2 and 3.0E-2 respectively.

## II. RESULTS

We simulate the muon collider spin precession for a grid of values of  $\hat{P} = -0.9, -0.74, -0.5$  and  $-0.26$  and fractional measurement error for the first turn (PERR) of 0.5E-2, 1.0E-2, 2.0E-2 and 3.0E-2. Figure 4(a) shows the result of the MINUIT fit plotted for 50 turns for  $\hat{P} = -0.26$  and  $\text{PERR} = 0.5\text{E-}2$ . Figure 4(b) shows the same plot but with the function being plotted only at integer values of the turn number  $t$ . A beat is evident in both the theoretical curve and the simulated measurements as a result of sampling the oscillation function at fixed intervals, not connected with the oscillation frequency. The origin of the beat is stroboscopic. Figure 4(c) shows the pulls, defined as  $(data - fit)/error$  at each measurement as a function of turn number for 1000 turns. There are no major turn dependent variations in this quantity indicating that the fit converged satisfactorily. Figure 4(d) shows the histogram of the pulls,

05/09/97 10.28

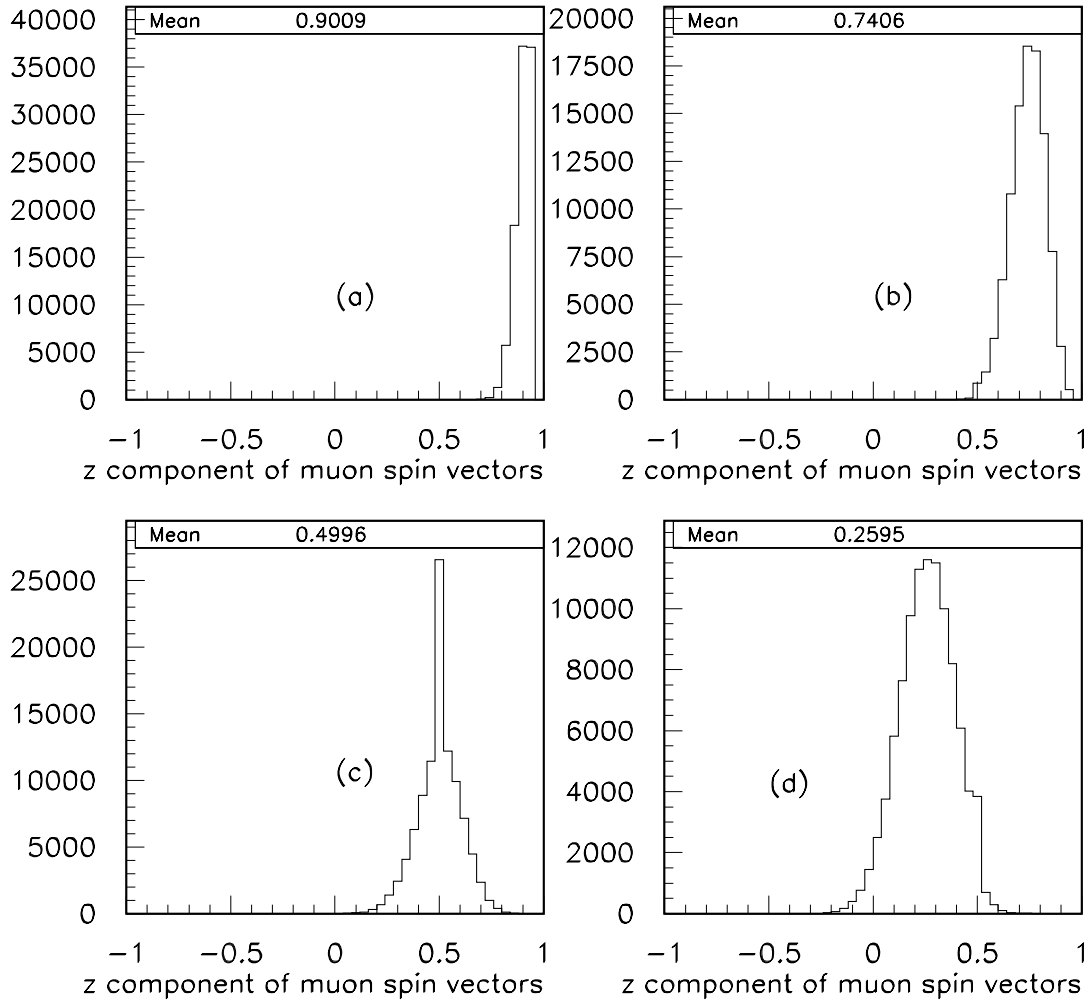


FIG. 3. (a)-(d) show the distribution of the z component of the spin vectors for the four samples considered.

which approximates a unit Gaussian as desired. Table II shows the results of the fit for the grid of values of  $\hat{P}$  and PERR. The results presented in table II are shown graphically in Figure 5. As an example, for an average polarization  $\hat{P} = -0.26$ , the fractional error in  $\delta\gamma/\gamma$  varies from 5.1E-6 to 1.9E-5 as the fractional error in the electron energy sampled varies from 0.5E-2 to 3.0E-2, corresponding to the number of electrons sampled during the first turn varying from 41261 to 1146. The average number of decays in the muon collider is expected to be 3.2E6 decays per meter for a beam intensity of  $10^{12}$  muons. The error in determining  $\gamma$  is thus going to be dominated by the fluctuations in the number of electrons sampled turn by turn, rather than sampling fluctuations in the calorimeter. We have simulated conditions involving  $\approx 40,000$  decays. It should be possible to go to higher statistical precision than computed here by sampling larger number of electrons.

The results for  $\delta\gamma/\gamma$  obtained from the measurement of the turn by turn rate of decay of the electron energy are not competitive with the precession method primarily because of the small value of  $\alpha$  (0.8399E-3). This leads to larger fractional errors for  $\gamma$  from this method (which also assumes that the loss of intensity is entirely due to the decay process) by almost three orders of magnitude than from the precession method.

#### A. Variation of $\delta\gamma/\gamma$ as a function of muon energy

The spin precession per turn equals  $2\pi$  for a  $\gamma$  value of 857.689, which corresponds to a muon beam momentum of 90.622 GeV/c. This is the first spin resonance for muons. At this point, the fitting method loses sensitivity completely, since there will be no spin oscillations turn by turn. We now study the error  $\delta\gamma/\gamma$  as a function of beam energy for  $\hat{P}=-0.26$  and PERR=0.5E-2 (keeping the magnetic field in the idealized storage ring to be 4.0 Tesla) as a function of muon beam energy that straddles the spin resonance. For initial muon collider physics, the interesting beam energies are 45.5 GeV (half the Z mass), 80.3 GeV ( $W$  threshold), 175 GeV (top threshold) as well as half the neutral Higgs mass, which could be as low as 55 GeV in some SUSY scenarios. We sample all electrons that have energies

$\hat{P}$	PERR	Number of electrons sampled	$\delta\gamma/\gamma_{oscillations}$	$\delta\gamma/\gamma_{decay}$	$\chi^2$ for NDF=1000
-0.90	0.50E-02	41261	0.14568E-05	0.13227E-02	824.
-0.90	0.10E-01	10315	0.22147E-05	0.20124E-02	936.
-0.90	0.20E-01	2579	0.39999E-05	0.36398E-02	1009.
-0.90	0.30E-01	1146	0.58659E-05	0.53457E-02	1030.
-0.74	0.50E-02	41261	0.17418E-05	0.13019E-02	843.
-0.74	0.10E-01	10315	0.26183E-05	0.19591E-02	954.
-0.74	0.20E-01	2579	0.46981E-05	0.35229E-02	1021.
-0.74	0.30E-01	1146	0.68765E-05	0.51672E-02	1039.
-0.50	0.50E-02	41261	0.25903E-05	0.12813E-02	888.
-0.50	0.10E-01	10315	0.38407E-05	0.19029E-02	973.
-0.50	0.20E-01	2579	0.68338E-05	0.33972E-02	1026.
-0.50	0.30E-01	1146	0.99744E-05	0.49749E-02	1041.
-0.26	0.50E-02	41261	0.51242E-05	0.12688E-02	898.
-0.26	0.10E-01	10315	0.75317E-05	0.18791E-02	1004.
-0.26	0.20E-01	2579	0.13324E-04	0.33447E-02	1053.
-0.26	0.30E-01	1146	0.19380E-04	0.48950E-02	1061.

TABLE II. Results of fits for  $\delta\gamma/\gamma$  as a function of polarization  $\hat{P}$  and noise PERR. Also shown is the  $\chi^2$  of the fit for 1000 turns.

greater than half the muon energy. Figure 6 shows the variation of  $\delta\gamma/\gamma$  as a function of muon beam energies that straddle these values. It can be seen that  $\delta\gamma/\gamma$  first decreases as one gets close to the resonance and then blows up on the spin resonance. Figures (7-11) show the fitted solutions superimposed on the simulated data for various momenta. Also shown side by side is the simulated data by itself. As one approaches the spin resonance, the oscillations slow down. It is nevertheless possible to fit the slowed down oscillations by a rapidly oscillating theoretical function to high accuracy on either side of the resonance. At the resonance, the oscillations die completely, which results in a large value of  $\delta\gamma/\gamma$ . It may be possible to use this blow-up in  $\delta\gamma/\gamma$  to find the spin resonance accurately and (paradoxically) determine  $\gamma$  at resonance accurately. This would depend on the width of the spin resonance, an analysis of which would take us beyond the scope of this paper.

### B. Variation of $\delta\gamma/\gamma$ as a function of beam energy spread

We now calculate the variation of polarization as a function of turn number for an ensemble of muons with initial value of polarization  $\hat{P} = -0.26$  and values of momentum spread  $\delta p/p$  varying from 0.02E-2 to 0.00125E-2. This variation is plotted in figure 13. For the larger values of momentum spread, there is a significant degradation of polarization as a function of turn number, due to differential spin precession of the individual beam particles. We note that when the beam energy is at 175 GeV, the spin tune is significantly higher and the depolarization is more rapid. Despite this depolarization, there is enough information from the first few hundred turns to extract the excellent value of  $\delta\gamma/\gamma$  for 175 GeV beam energy as shown in figure 6.

Figure 14 shows the variation of the fractional energy resolution,  $\delta\gamma/\gamma$  as a function of fractional beam energy spread for a muon beam with  $\hat{P} = -0.26$ , with 41261 electrons sampled. There is little dependence of  $\delta\gamma/\gamma$  on the momentum spread. This is due to the fact that the momentum spread is determined from the spin tune and not from the spin oscillation amplitude and the fact that the depolarization is not significant for the first few

hundred turns for any of the beam momentum spreads considered here.

### C. Optimization of the electron energy cut

We now vary the cut on electron energy and study the dependence on  $\delta\gamma/\gamma$  on the cut. Figure 15 shows the variation of  $\delta\gamma/\gamma$  with the cut on individual electron energies for  $\hat{P} = -0.26$  for 41261 and 1146 electrons sampled. As shown in the Appendix, the fractional error on the average energy of electrons is much smaller than the fractional error on the total energy of electrons. It is possible to measure the average electron energy by counting the number of electrons going into the calorimeter with a scintillator array. However, the precession information is contained increasingly in the number of electrons rather than their average energy as we increase the electron energy cut. Figure 15 shows the variation of  $\delta\gamma/\gamma$  calculated from average as well as total electron energy as a function of the electron energy cut. For smaller values of the electron energy cut, the average method produces superior errors than the total energy method. However, with 40,000 electrons or more sampled a total energy method with a cut of 25 GeV or higher seems optimal. It should however be pointed out that the average energy method does not require a model for the rate of decay of muon intensity in the machine, which in practice could be a complicated function of turn number. As such the systematics associated with this would not be present in the average energy method. Figure 16(a) shows the variation of the absolute value of  $C/F$  as a function of the electron energy cutoff for  $\hat{P} = -0.26$ , where  $C$  and  $F$  are defined in equation 1.10 for both the total energy method and the average energy method. Figure 16(b) shows the fraction of electrons that lie above the electron energy cut as a function of the energy cut. The polarization for this sample is 0, since the electron energy fraction depends on polarization as well. Given the curves shown in figure 16, it should be possible to estimate the error in  $\delta\gamma/\gamma$  for a variety of conditions.

### III. EFFECTS DUE TO DEPARTURES FROM THE IDEAL CASE

So far we have considered a planar collider ring with uniform vertical magnetic field and no electric fields. The actual collider ring will depart from the ideal in three respects; a) It will have RF electric fields to keep the muons bunched, b) it will have radial horizontal magnetic fields experienced by particles in an off-center trajectory at quadrupoles and at vertical correction dipoles, and c) it will have longitudinal magnetic fields due to solenoidal magnets in the interaction region(s). We now consider the effect due to each of these departures from the ideal.

#### A. Electric fields

Equation 1.2 implies that there is no spin precession due to longitudinal electric fields ( $\vec{\beta} \times \vec{E} = 0$ ). RF electric fields are longitudinal, so there will be no precession due to the RF electric fields. At present there are no plans to install electrostatic separators to separate the beams. If and when this happens, one should consider the effect due to the transverse electric fields thus introduced.

#### B. Effect of radial magnetic fields

Particles which are off-axis at quadrupoles will experience radial as well as vertical magnetic fields. Even though the net integral of these off-axis fields around the ring is zero, the spin rotation along a horizontal axis followed by spin rotation about a vertical axis (caused by a bend dipole) followed by a reverse rotation in the horizontal direction still produces a net effect since the rotations about the horizontal and vertical axes do not commute. The effects have been analyzed by Assmann and Koutchouk [5] who show that this results in both a net spin tune shift  $\langle \delta\nu \rangle$  as well as a spread in tune  $\sigma_{\delta\nu}$ .

$$\langle \delta\nu \rangle = \frac{cot\pi\nu_0}{8\pi} \nu_0^2 \left( n_Q (Kl_Q)^2 \sigma_y^2 + n_{CV} \sigma_{\theta CV}^2 \right) \quad (3.1)$$

where  $\nu_0 \equiv a\gamma$  is the spin tune of the collider ring,  $n_Q$  are the number of quadrupoles with integrated gradient  $Kl_Q$ ,  $\sigma_y$  is the misalignment spread of the closed orbit at the quadrupoles,  $n_{CV}$  is the number of vertical correction dipoles and  $\sigma_{\theta CV}$  is the rms beam angle in the vertical correctors. The spread in tune is given by,

$$\sigma_{\delta\nu} = \frac{\langle \delta\nu \rangle}{\cos\pi\nu_0} \quad (3.2)$$

Table III shows the values for  $\langle \delta\nu \rangle$  and  $\sigma_{\delta\nu}$  obtained by Assman and Koutchuk [5] for LEP. We compare this with to the current design for the 50 GeV muon collider ring [6]. Including the low beta section, there are 70 quadrupoles with an RMS value of  $Kl_Q = 0.27 \text{ m}^{-1}$ . The effects due to correction dipoles may be neglected in both the LEP and the muon collider cases. We assume a beam misalignment of 5mm at the quadrupoles, which is the same value used in the LEP calculation. This is probably being conservative. The tune shift for LEP corresponds to a shift in beam energy calibration of 3.0 KeV. The tune spread for LEP corresponds to a spread in beam energy calibration of 30 KeV. For the muon collider, the tune shift corresponds to a shift in beam energy calibration of -0.24 KeV and a spread of 1.46 KeV, both of which are negligible. The reason for the smallness of this effect for the muon collider is twofold. Since the circumference of the muon collider is smaller than LEP, there are fewer quadrupoles. Secondly, the muon is two hundred times more massive than the electron and has a spin tune  $a\gamma$  that is smaller by the same factor. The spin tune shift depends on the the square of the spin tune. It should be noted that the above formulae are not valid for a fractional spin tune of 0.5.

### C. Solenoidal magnetic fields

The experimental region will in all likelihood contain a solenoidal magnet. This solenoidal field, if uncorrected, will rotate the spin vector of the muons about the beam direction by a constant amount  $\theta_s$  per turn, which can be derived using equation 1.2.

$$\theta_s = -\frac{e}{\gamma m_\mu}(1+a)B_s = -(1+a)\frac{B_s l}{B\rho} \quad (3.3)$$

where  $B_s$  is the field due to the solenoid of length  $l$ ,  $B$  is the dipole bending field of the ring of radius  $\rho$ . For a solenoid of 1.5 Tesla and length 6 meters,  $\theta_s = 3.09$  degrees for the planar storage ring parameters of table I. It can be shown analytically [8] that this produces a spin tune shift  $\delta\nu$  given by

$$\nu + \delta\nu = \frac{1}{\pi} \arccos \left( \cos(\pi\nu) \cos\left(\frac{\theta}{2}\right) \right) \quad (3.4)$$

yielding a spin tune shift  $\delta\nu = -1.901\text{E-}5$ , or a fractional spin tune shift of  $\delta\nu/\nu = -3.45\text{E-}5$ . For a 50 GeV muon beam, this is a shift in energy calibration of -1.72 MeV. In LEP, a similar solenoid will have a much smaller fractional tune shift [8], since the tune is 200 times larger for electrons. It is important to correct the effect due to the solenoids, since this is cumulative turn by turn. At LEP this is done by a series of vertical orbit correctors [9] followed by normal lattice followed by vertical orbit correctors of reverse polarity, which has the effect of rotating the spin by half the amount produced by the solenoid. A similar set of corrections is inserted after the solenoid to complete the correction. This method depends on a non-zero value of  $g - 2$  and as such will be 200 times less effective for muons than for electrons, for any given magnet strength. The most effective method to correct for the solenoid is to surround it on either side by compensating solenoids of minimal radius large enough to allow the beam to go through.

#### IV. CONCLUSIONS

We have demonstrated that it is feasible to measure the energy of a 50 GeV muon collider to a few parts per million using the  $g - 2$  spin precession technique, provided it is feasible to maintain a muon polarization of the order of  $\hat{P}=0.25$  in the ring for a thousand turns. In order to explore the Higgs resonance, it is necessary to measure the bunch by bunch variation in energy to a few parts per million. We have demonstrated that the  $g - 2$  technique is capable of doing so. It is still possible to tolerate a spin tune shift in the overall energy scale of a few percent, which will act only as a systematic error on the Higgs mass and width.

We would also like to note in passing that polarization information from a calorimeter of the type proposed here can be used in conjunction with a neutrino detector placed along the line of the neutrinos produced in association with the electrons to estimate the variation in the energy spectrum of the muon neutrinos and electron antineutrinos in the beam. Such information can be a valuable tool in untangling various possible neutrino oscillation scenarios.

We intend to develop the method here by studying the propagation of polarized muons in a realistic 50 GeV collider lattice using the program COSY [7] that takes into account non-linear effects in the dynamic aperture. Design and Monte Carlo studies will also be undertaken to develop the calorimeter detector needed. The authors would like to acknowledge useful conversations with Alain Blondel, Yaroslav Derbenev and Robert Rossmanith.

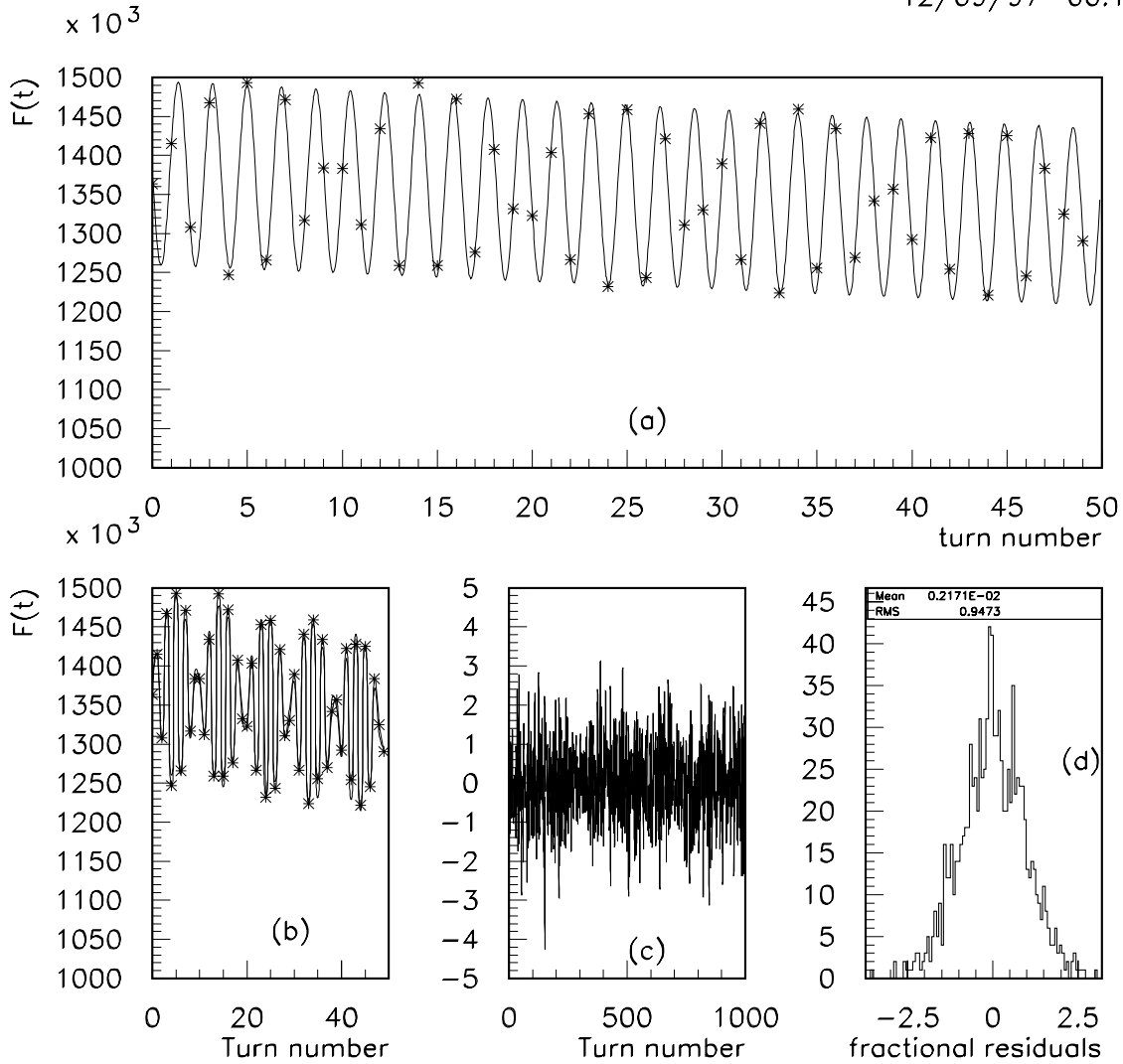


FIG. 4. (a) Energy detected in the calorimeter during the first 50 turns in a 50 GeV muon storage ring (points). An average value of  $\hat{P} = -0.26$  is assumed and a fractional fluctuation of  $0.5E-2$  per point. The curve is the result of a MINUIT fit to the functional form in equation 1.10. (b) The same fit, with the function being plotted only at integer turn values. A beat is evident. (c) Pulls as a function of turn number (d) Histogram of pulls.

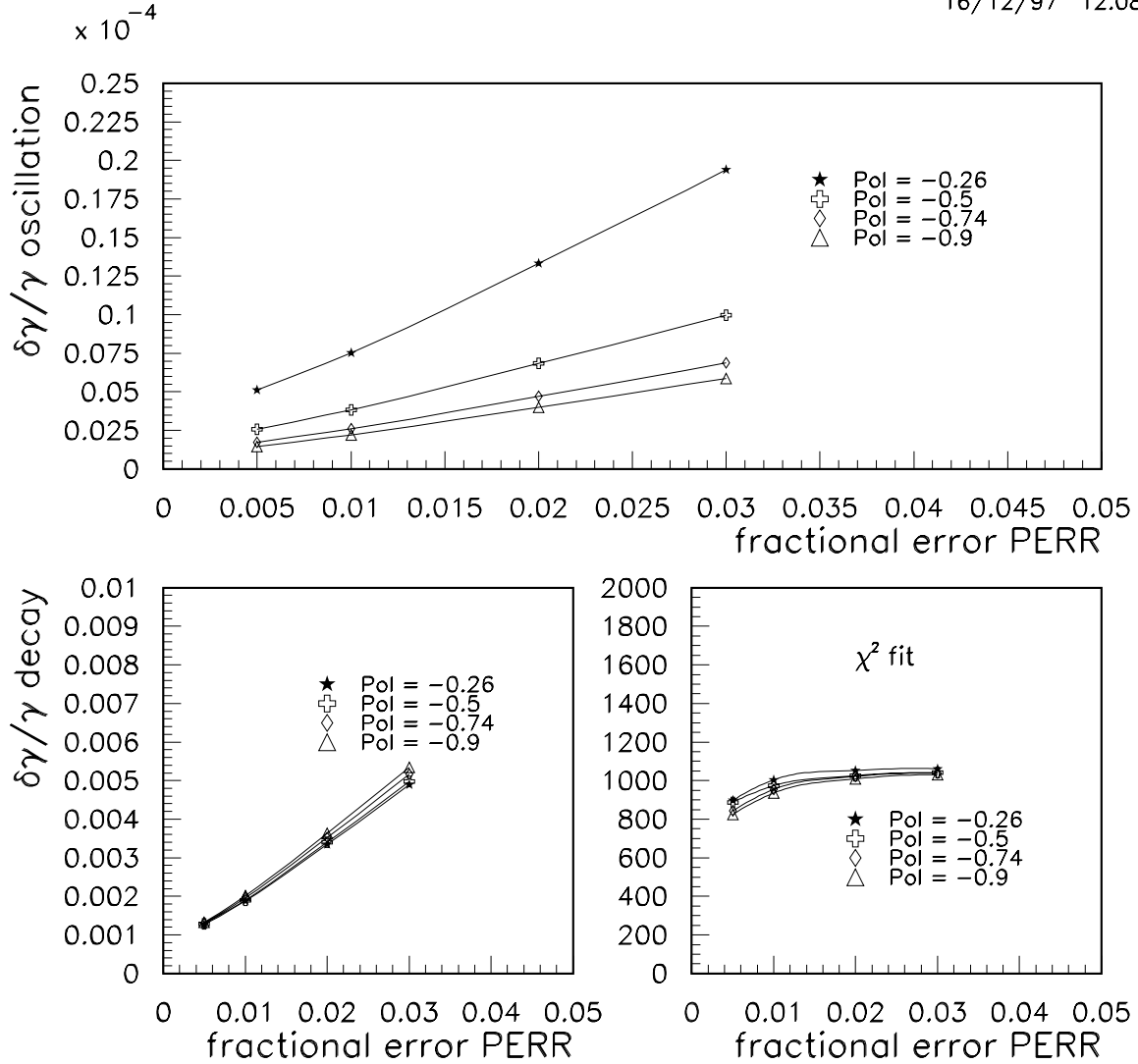


FIG. 5. (a) Fractional error in  $\delta\gamma/\gamma$  obtained from the oscillations as a function of polarization  $\hat{P}$  and the fractional error in the measurements PERR (b) Fractional error in  $\delta\gamma/\gamma$  obtained from the decay term as a function of polarization  $\hat{P}$  and the fractional error in the measurements PERR (c) The total  $\chi^2$  of the fits for 1000 degrees of freedom

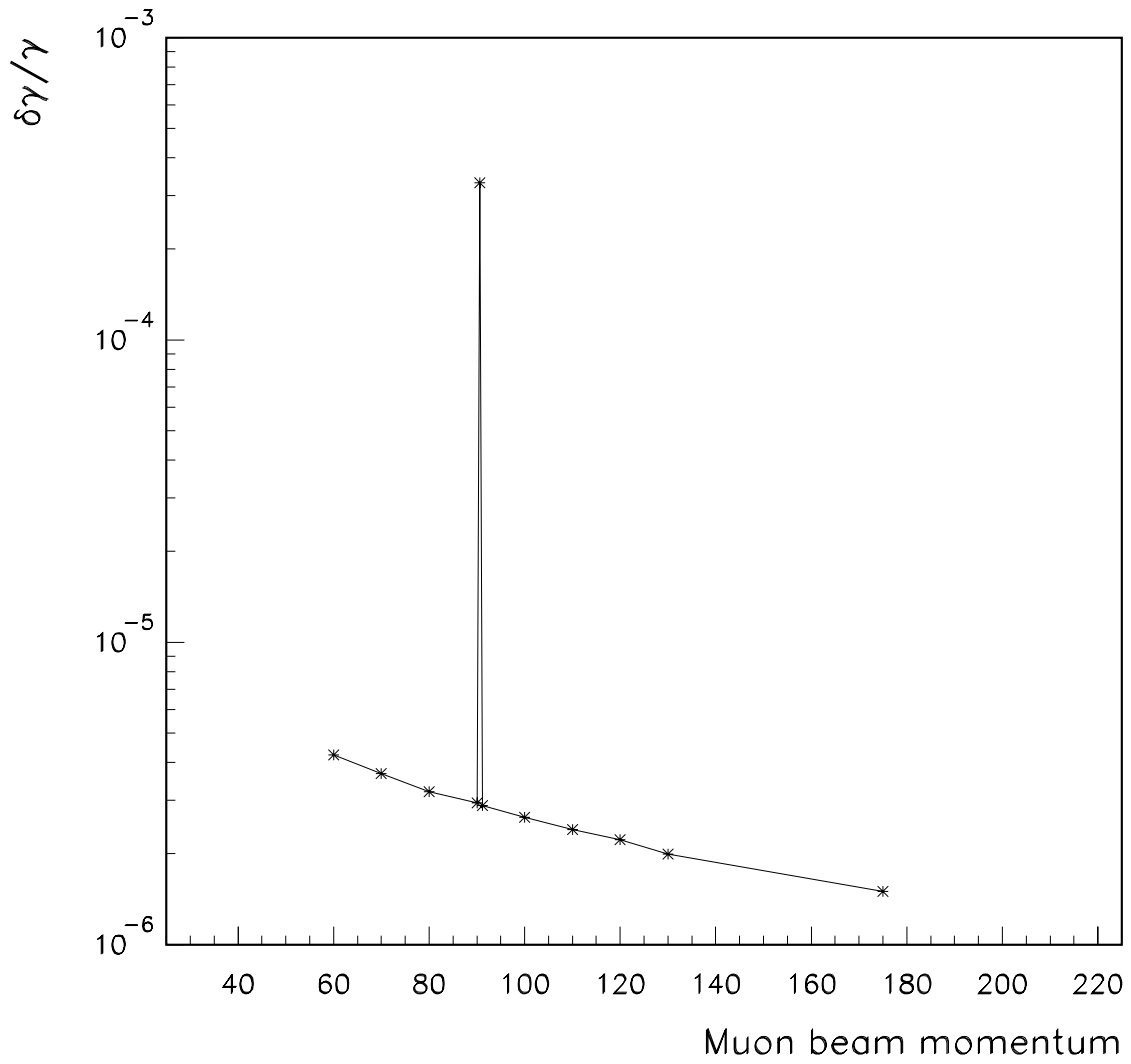


FIG. 6. Fractional error in  $\delta\gamma/\gamma$  obtained from the oscillations as a function of muon beam momentum

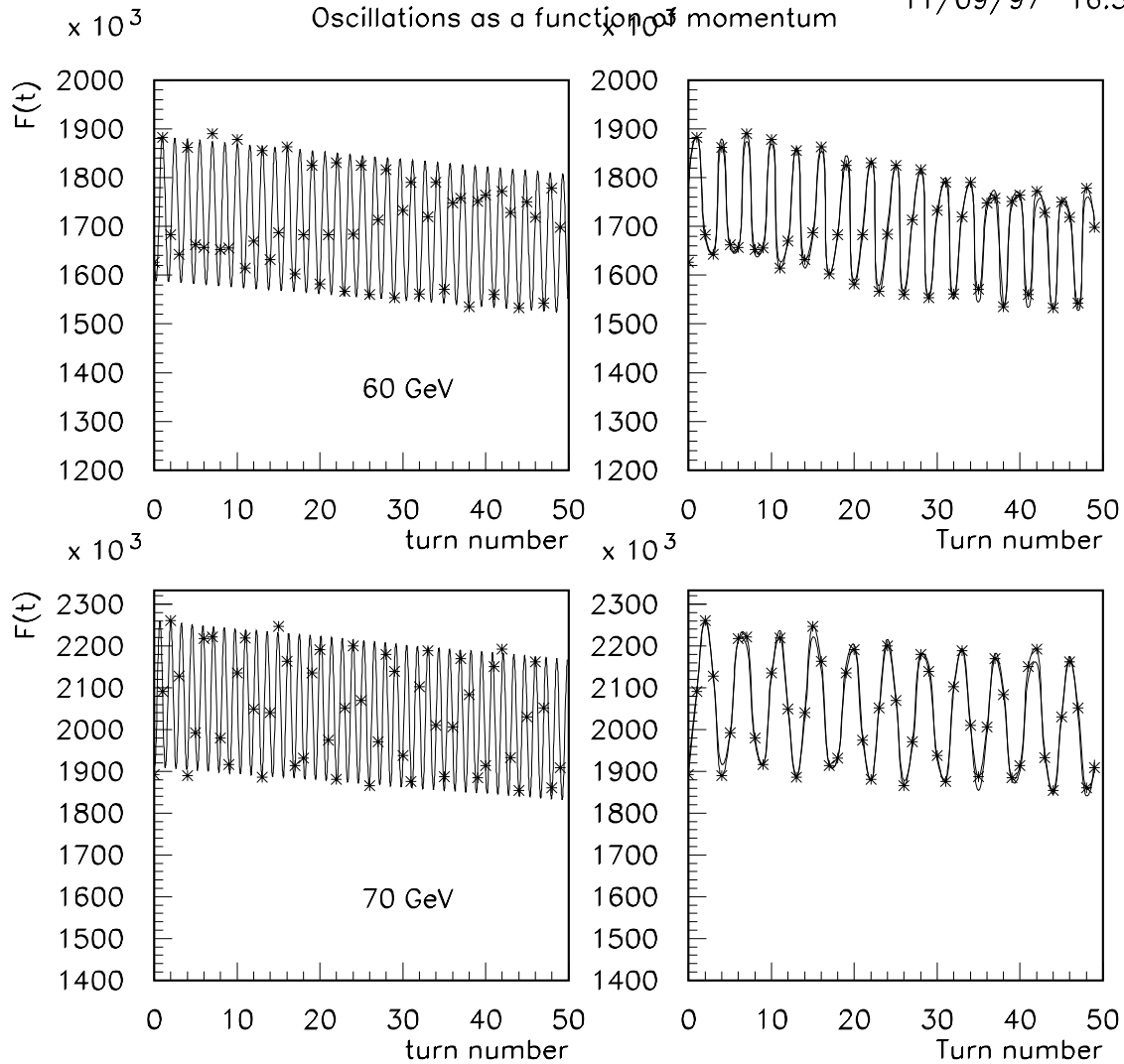


FIG. 7. The figures on the left hand side show the simulated data with the fitted function superimposed for 50 turns. The figures on the right hand side show the simulated data and the fitted function at integer values of the turn number. The data shown are 60 GeV/c and 70 GeV/c muon momenta respectively.

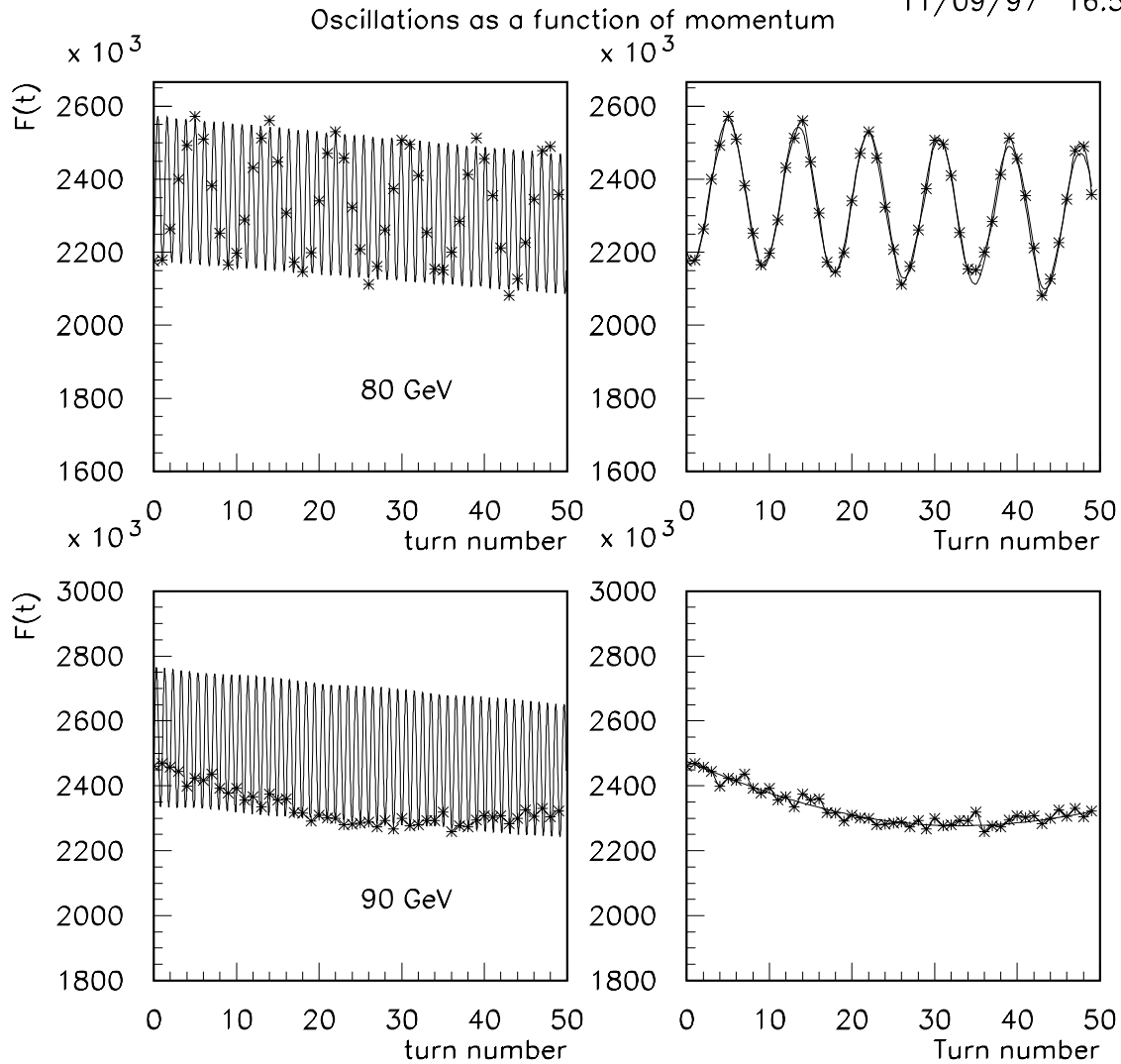


FIG. 8. The figures on the left hand side show the simulated data with the fitted function superimposed for 50 turns. The figures on the right hand side show the simulated data and the fitted function at integer values of the turn number. The data shown are 80 GeV/c and 90 GeV/c muon momenta respectively.

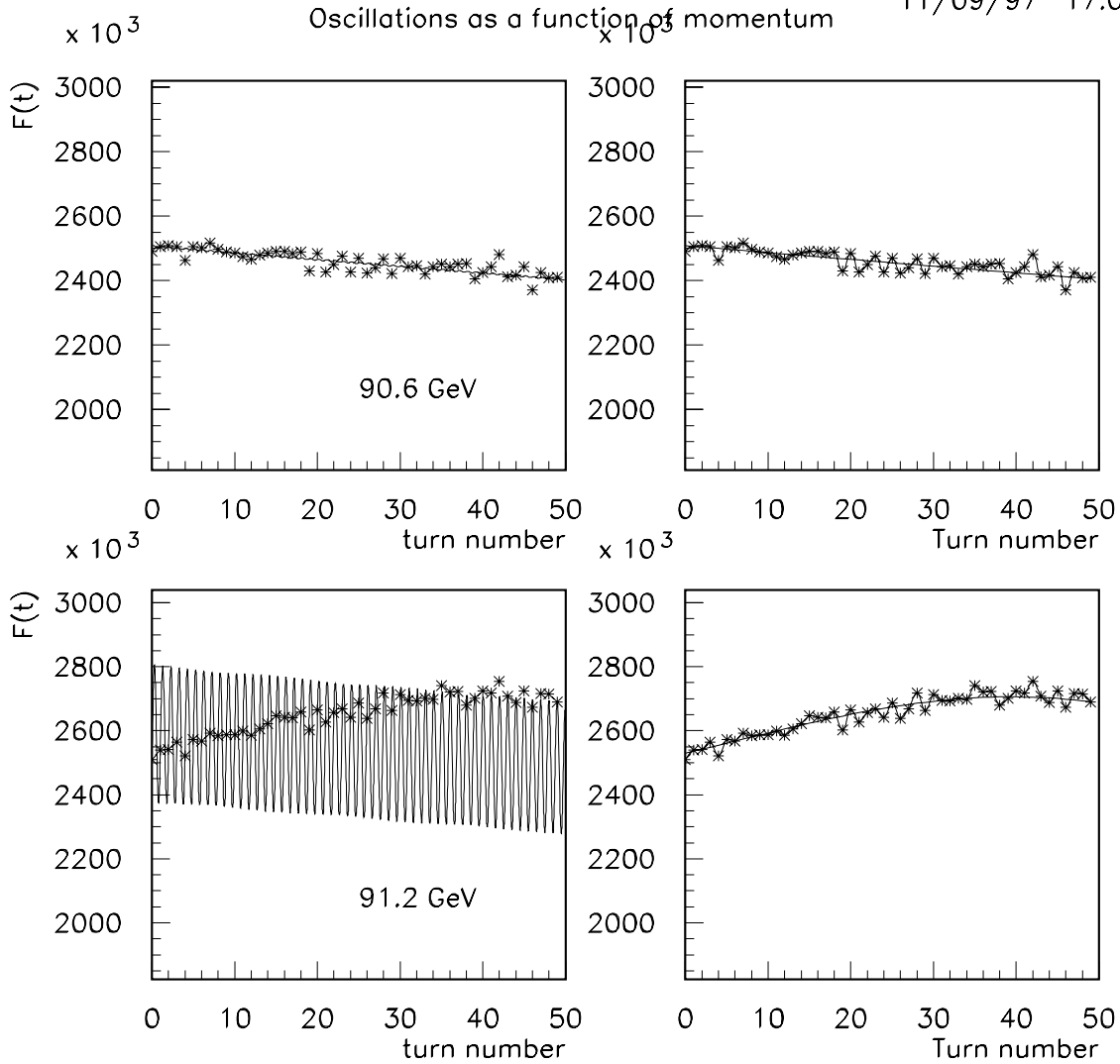


FIG. 9. The figures on the left hand side show the simulated data with the fitted function superimposed for 50 turns. The figures on the right hand side show the simulated data and the fitted function at integer values of the turn number. The data shown are 90.622 GeV/c and 91.2 GeV/c muon momenta respectively. The upper curve is on resonance.

## Oscillations as a function of momentum

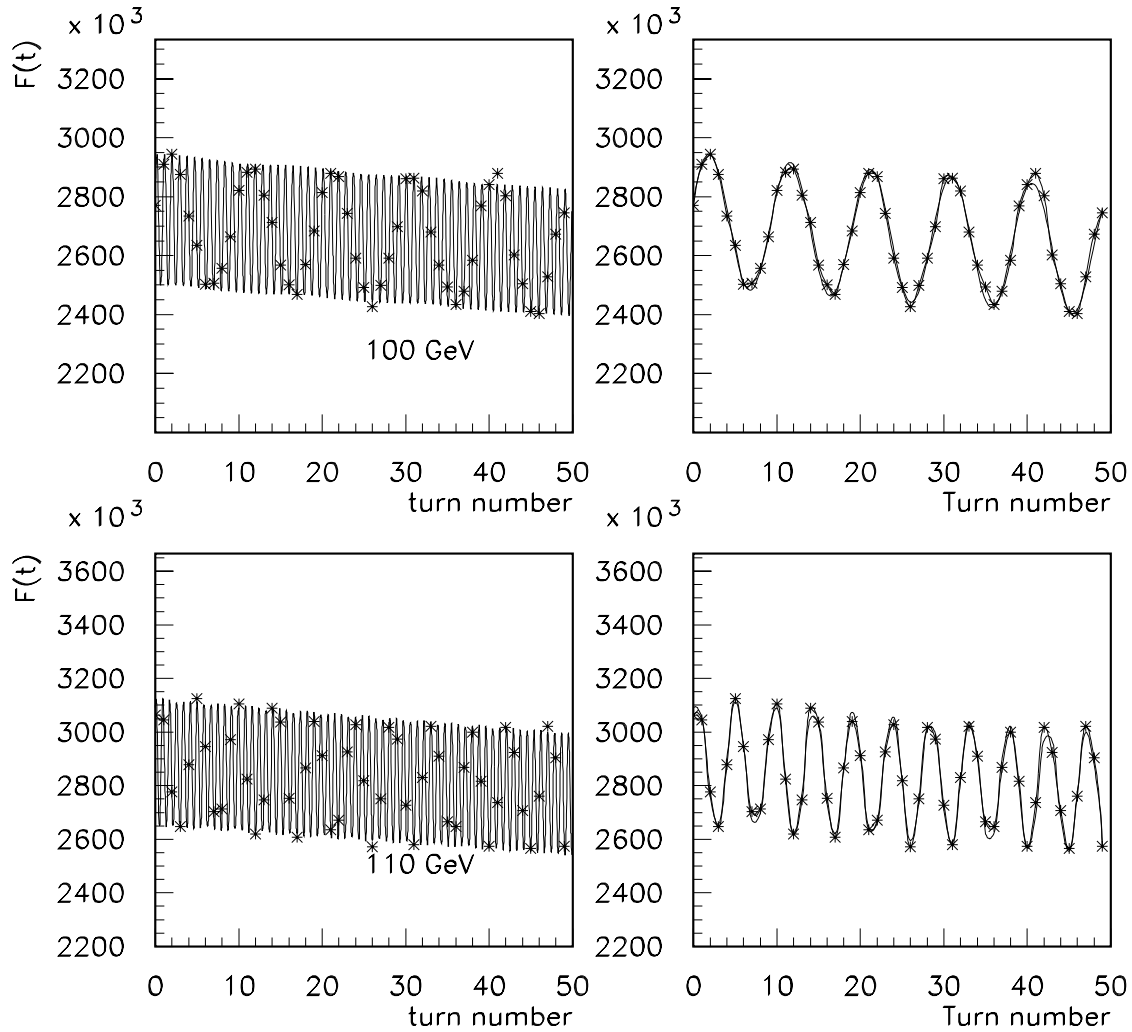


FIG. 10. The figures on the left hand side show the simulated data with the fitted function superimposed for 50 turns. The figures on the right hand side show the simulated data and the fitted function at integer values of the turn number. The data shown are 100 GeV/c and 110 GeV/c muon momenta respectively.

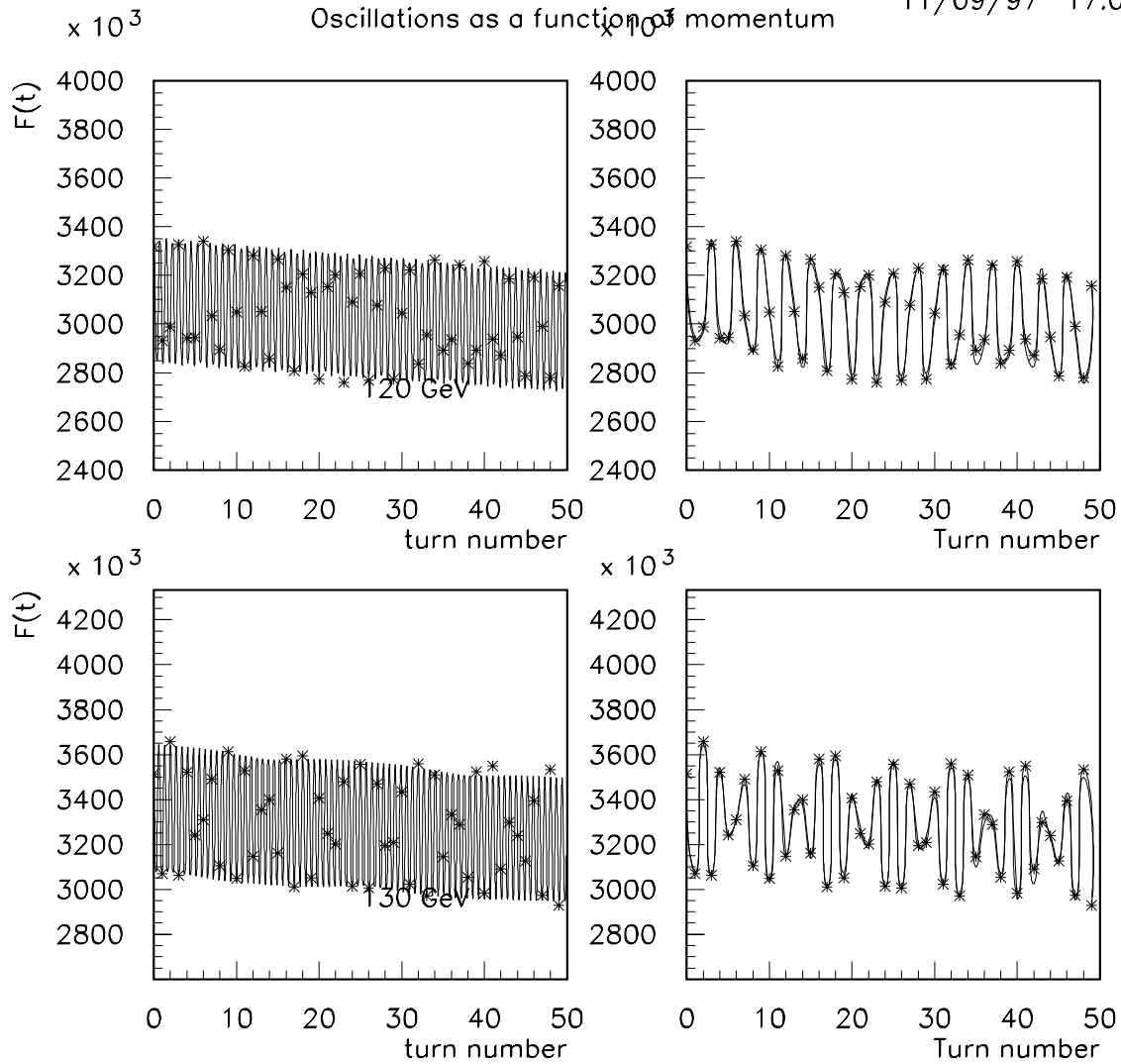


FIG. 11. The figures on the left hand side show the simulated data with the fitted function superimposed for 50 turns. The figures on the right hand side show the simulated data and the fitted function at integer values of the turn number. The data shown are 120 GeV/c and 130 GeV/c muon momenta respectively.

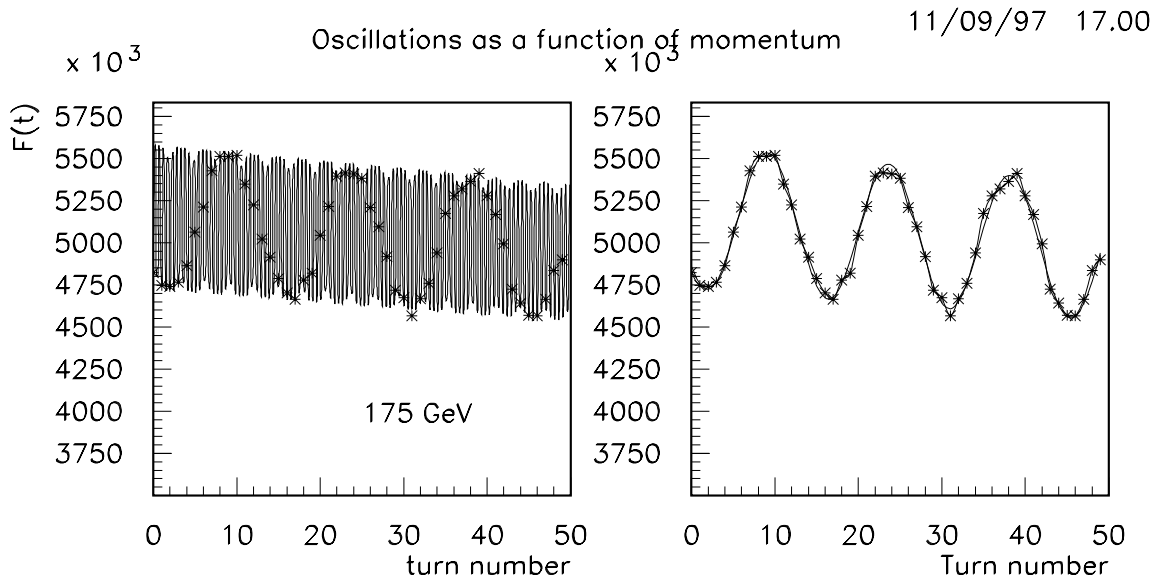


FIG. 12. The figures on the left hand side show the simulated data with the fitted function superimposed for 50 turns. The figures on the right hand side show the simulated data and the fitted function at integer values of the turn number. The data shown are 175 GeV/c muon momentum.

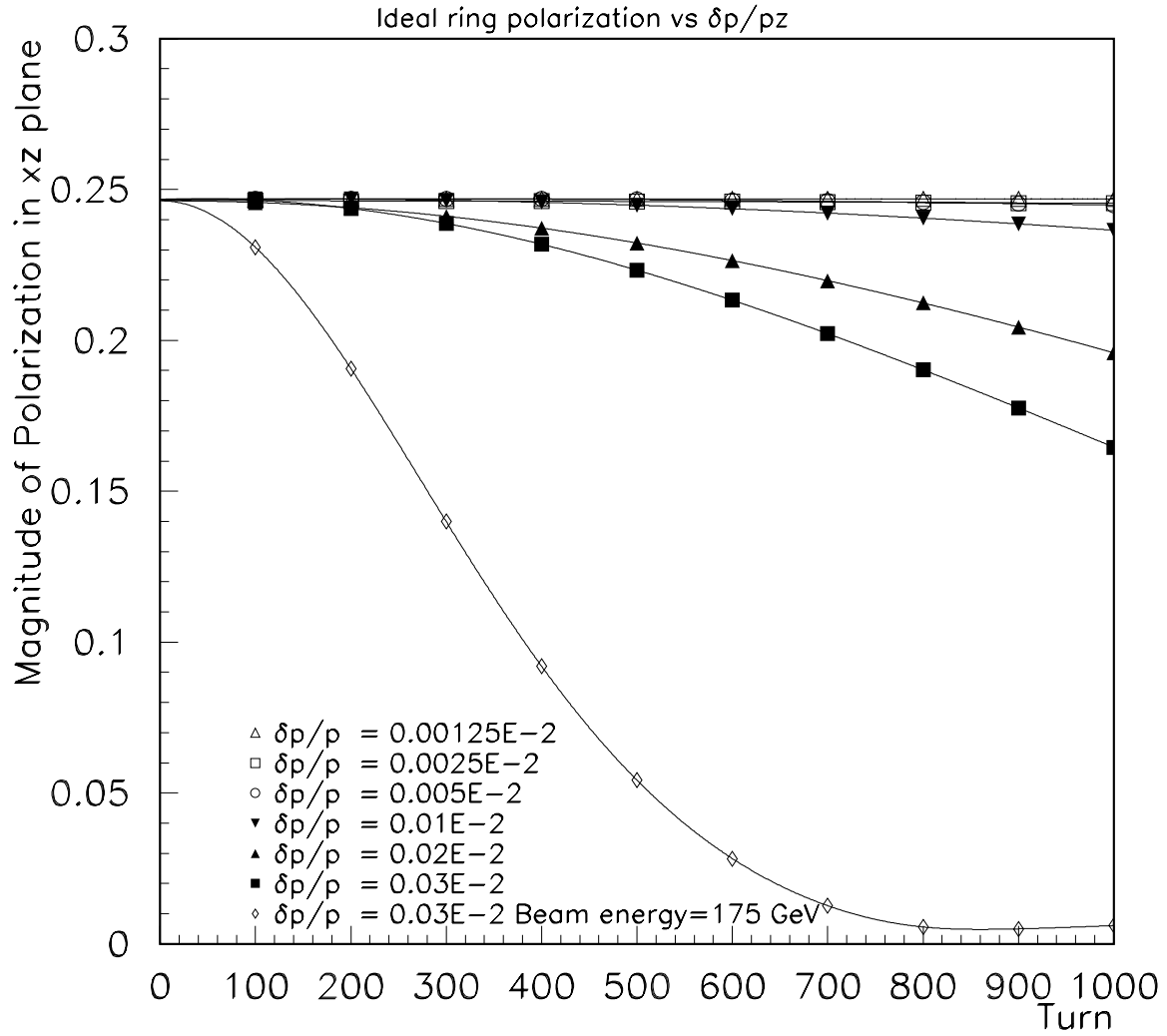


FIG. 13. Variation of polarization as a function of turn number for 50 GeV muons with initial  $\hat{P} = -0.26$  and various values of  $\delta p/p$  in an ideal collider ring. The bottom curve is for 175 GeV muons and shows a more rapid depolarization due to the higher spin tune.

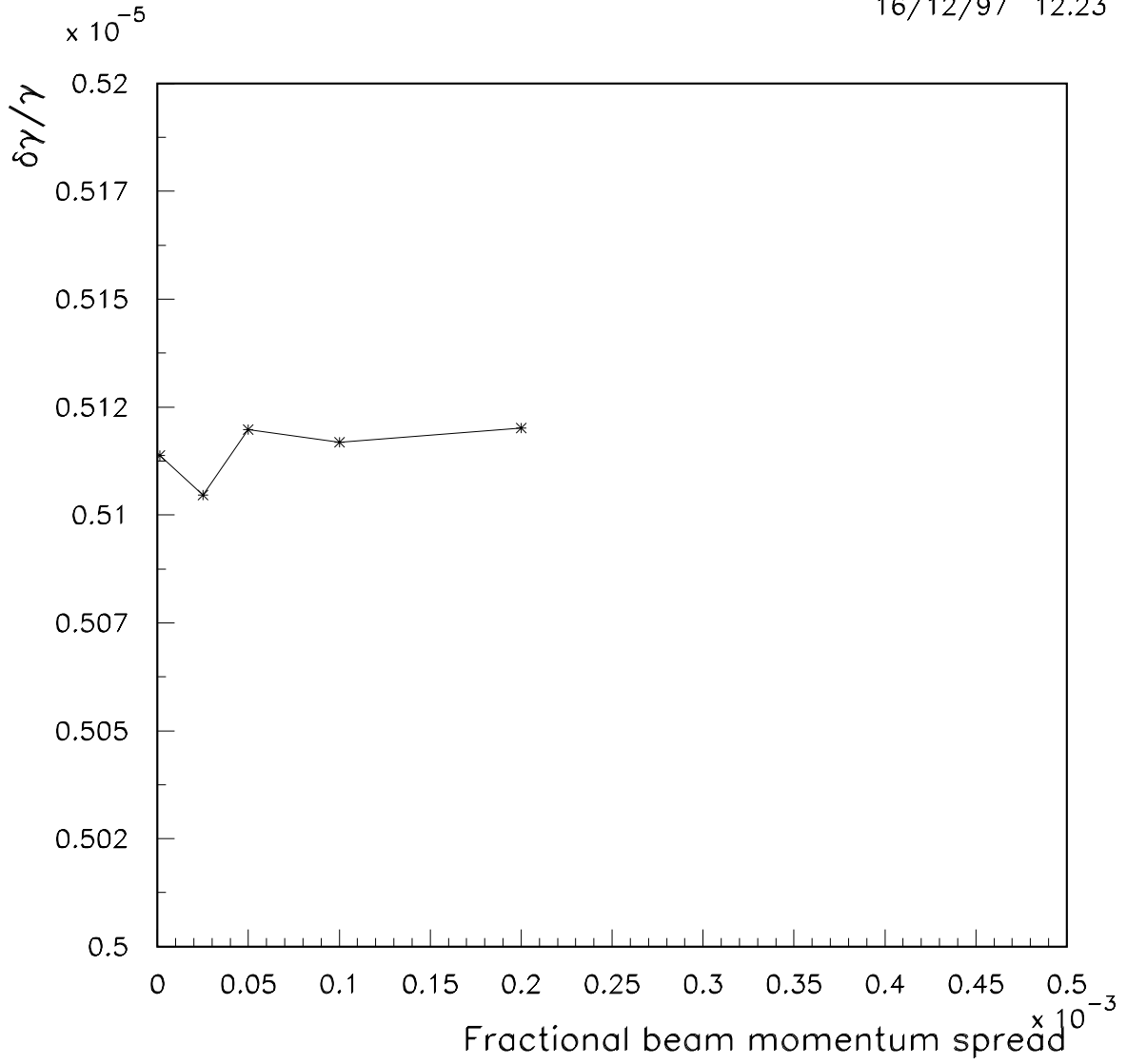


FIG. 14.  $\delta\gamma/\gamma$  versus fractional beam energy spread for 50 GeV muons with  $PERR=.5E-2$  and  $\hat{P} = -0.26$

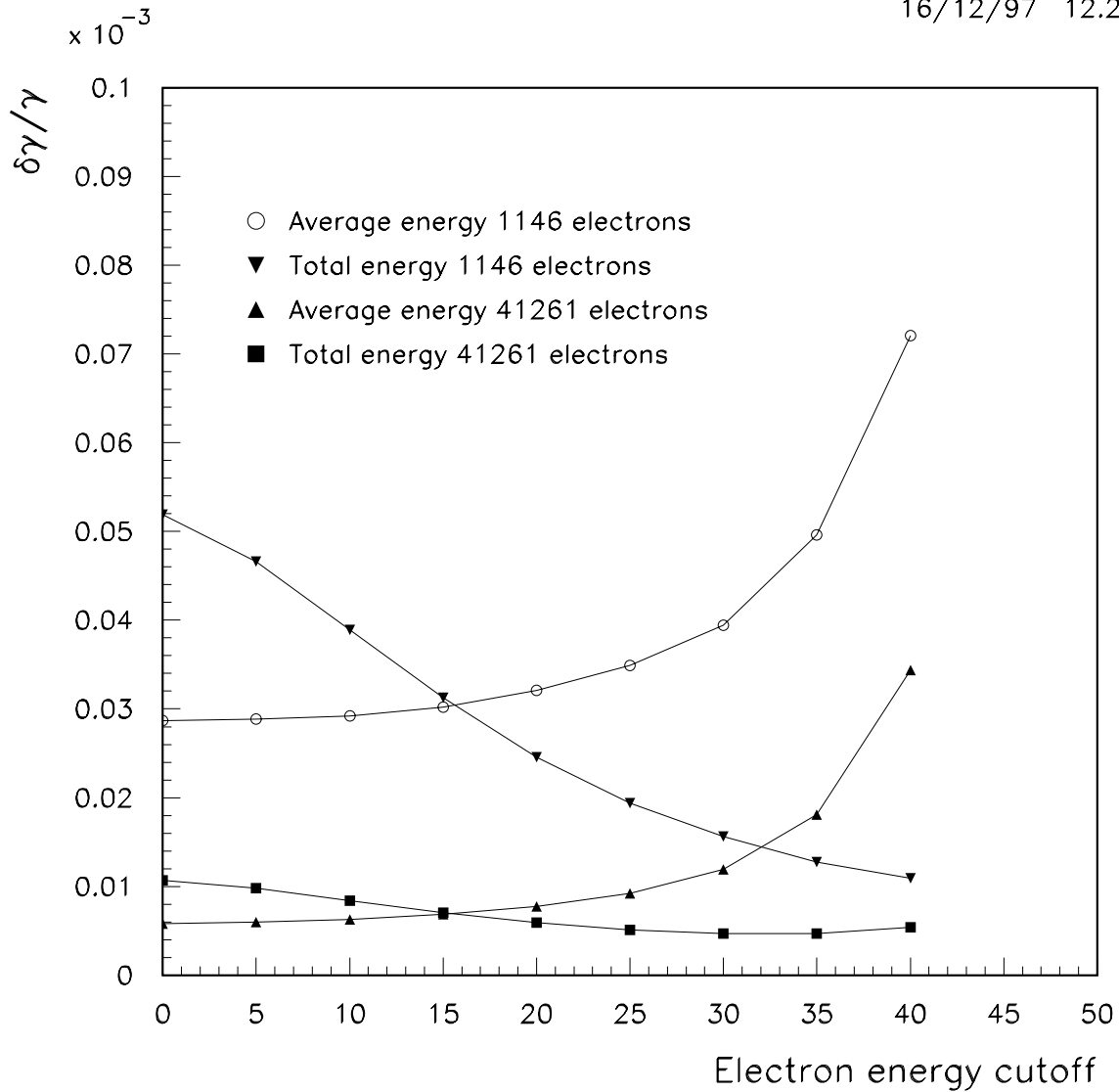


FIG. 15. The variation of  $\delta\gamma/\gamma$  as a function of the electron energy cut for 41261 and 1146 electrons  $\hat{P} = -0.26$ . We fit the total energy in the calorimeter as well as the average energy per electron

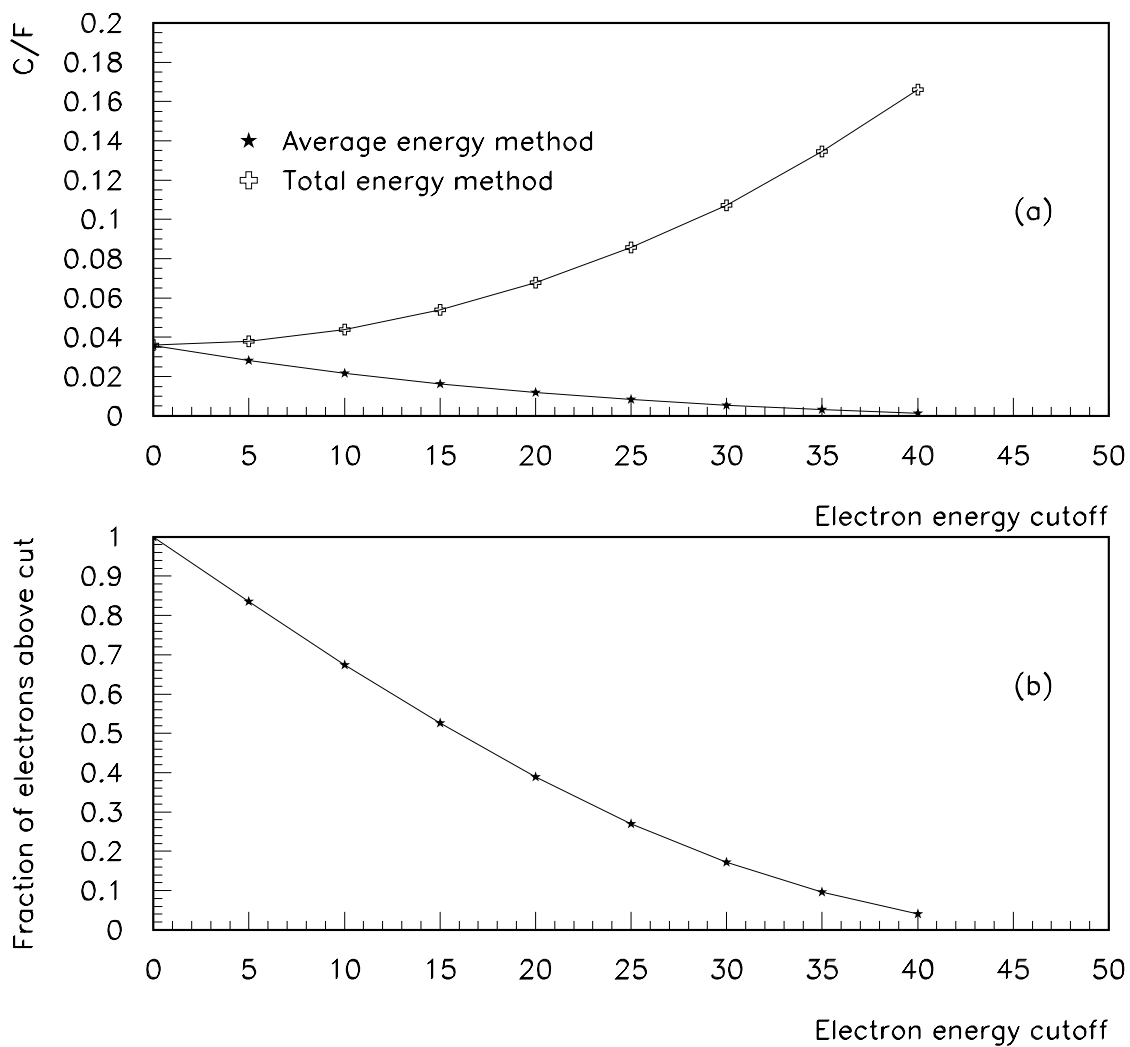


FIG. 16. (a) The variation of  $C/F$  as a function of the electron energy cut for  $\hat{P} = -0.26$  for total energy method and average energy method. (b) The fraction of electrons that survive the energy cut as a function of the cut for  $\hat{P} = 0$ .

## V. APPENDIX

### A. Treatment of Errors

We measure the total energy  $E$  of all electrons with individual energy  $e > 25$  GeV in an electromagnetic calorimeter. Let  $N$  be the number of electrons sampled during a turn.  $N$  can fluctuate from sampling to sampling. Then

$$E = \sum_{i=1}^N e_i = N \langle e \rangle \quad (5.1)$$

$$\frac{\sigma_E^2}{\langle E \rangle^2} = \frac{\sigma_N^2}{\langle N \rangle^2} + \frac{\sigma_{\langle e \rangle}^2}{\langle e \rangle^2} = \frac{1}{\langle N \rangle} \left( 1 + \frac{\sigma_e^2}{\langle e \rangle^2} \right) \quad (5.2)$$

where the variance  $\sigma^2$  of the quantities  $e$  and  $E$  results from the kinematic distributions of those quantities and not from the measurement errors. The average of the individual electron energies is denoted by  $\langle e \rangle$ .

Let the calorimeter be such that it measures the true deposited energy  $E$  with a resolution  $\epsilon(E)$  such that

$$\frac{\epsilon^2}{E^2} = \mathcal{C}^2 + \frac{\mathcal{S}^2}{E} + \frac{\mathcal{N}^2}{E^2} \quad (5.3)$$

where  $\mathcal{C}$ ,  $\mathcal{S}$  and  $\mathcal{N}$  represent the Constant, Sampling and Noise terms respectively. Let us assume that the measurement errors are Gaussian. Then,

$$P(E_m) = \int P(E)G(E, E_m, \epsilon)dE \quad (5.4)$$

where  $E_m$  is the measured energy and  $G(E, E_m, \epsilon)$  is a Gaussian of mean  $E$  and standard deviation  $\epsilon$ , which is a function of  $E$  and is written as  $\epsilon(E)$ . From this it follows that the mean measured energy  $\langle E_m \rangle$  and the mean squared measured energy  $\langle E_m^2 \rangle$  are given by

$$\begin{aligned} \langle E_m \rangle &= \int E_m P(E_m) dE_m = \int E_m dE_m \int P(E) G(E, E_m, \epsilon) dE \\ &= \int P(E) dE \int E_m G(E, E_m, \epsilon) dE_m = \int P(E) dE \times E = \langle E \rangle \end{aligned} \quad (5.5)$$

The equation 5.5 states that the mean value of any distribution given by  $P(E)$  is the same as that of the smeared distribution  $P(E_m)$  provided the smearing function is such that

the average of the smeared values for any given true value  $E$  equals the true value ( a property satisfied by Gaussians) and the integration is carried over the full range of the variables. As an aside, in High Energy Physics, we measure steeply falling spectra that are smeared by measurement errors. Provided there is no arbitrary lower cut-off in the measured spectra (such as a trigger threshold), the above result would be valid, even for non-Gaussian resolutions. For the muon collider, the cut off in selected electrons of 25 GeV is imposed by momentum selection that is independent of the calorimetry. So the above result would still be valid. Similarly, one can compute  $\langle E_m^2 \rangle$

$$\begin{aligned} \langle E_m^2 \rangle &= \int E_m^2 P(E_m) dE_m = \int E_m^2 dE_m \int P(E) G(E, E_m, \epsilon) dE \\ &= \int P(E) dE \int E_m^2 G(E, E_m, \epsilon) dE_m = \int P(E) dE \times (E^2 + \epsilon^2) = \langle E^2 \rangle + \int P(E) \epsilon^2(E) dE \end{aligned} \quad (5.6)$$

From this it follows that the variance of the measured energy  $\sigma_{E_m}^2$  is given by

$$\sigma_{E_m}^2 = \sigma_E^2 + \int P(E) \epsilon^2(E) dE \approx \sigma_E^2 + \epsilon^2(\langle E \rangle) \quad (5.7)$$

where the last approximation results from assigning the average measurement resolution to the resolution at the average energy. This then leads to

$$\frac{\sigma_{E_m}^2}{\langle E_m \rangle^2} \approx \frac{\sigma_E^2}{\langle E \rangle^2} + \frac{\epsilon^2(\langle E \rangle)}{\langle E \rangle^2} \quad (5.8)$$

Using equation 5.2 and 5.3 leads to

$$\frac{\sigma_{E_m}^2}{\langle E_m \rangle^2} \approx \frac{1}{N} \left( 1 + \frac{\sigma_e^2}{\langle e \rangle^2} \right) + \mathcal{C}^2 + \frac{\mathcal{S}^2}{N \langle e \rangle} + \frac{\mathcal{N}^2}{N^2 \langle e \rangle^2} \quad (5.9)$$

From the above equation, it is obvious that the calorimeter must be such that the constant term  $\mathcal{C}$  must be negligible for the fractional resolution to scale inversely with the number  $N$  of electrons collected. The noise term can be neglected for large enough  $N$  since it goes as  $N^{-2}$ . With these assumptions, one gets

$$\frac{\sigma_{E_m}^2}{\langle E_m \rangle^2} \approx \frac{1}{N} \left( 1 + \frac{\sigma_e^2}{\langle e \rangle^2} + \frac{\mathcal{S}^2}{\langle e \rangle} \right) \quad (5.10)$$

For a 50 GeV muon beam, the values of  $\langle e \rangle$  and  $\sigma_e$  are 34.05 GeV and 6.046 GeV respectively for electrons with  $e > 25$  GeV. The ratio,  $\sigma_e / \langle e \rangle$  is to a good approximation independent of muon energy. This then leads to the following error formula.

$$\frac{\sigma_{E_m}^2}{\langle E_m \rangle^2} \approx \frac{1}{N} \left( 1 + 0.03153 + \frac{S^2}{34.05} \right) \quad (5.11)$$

Sampling terms of  $0.15 \text{ GeV}^{1/2}$  or better are easy to obtain in electromagnetic calorimeters.

This leads to

$$\frac{\sigma_{E_m}^2}{\langle E_m \rangle^2} \approx \frac{1}{N} (1 + 0.03153 + 0.000661) \quad (5.12)$$

i.e. the sampling term can be neglected when compared to the fluctuation in the true electron energies. So if the fractional measurement error is  $\text{PERR} \equiv \frac{\sigma_{E_m}}{\langle E_m \rangle}$  is specified, the equivalent number of electrons is given by

$$N \approx \frac{1.03153}{(\text{PERR}^2)} \quad (5.13)$$

In other words,  $\text{PERR}= .5\text{E-}2, 1.0\text{E-}2, 2.0\text{E-}2$  and  $3.0\text{E-}2$  implies 41261, 10315, 2579, and 1146 electrons sampled. If in practice we sample 100,000 electrons, this leads to a value of  $\text{PERR}=0.3212\text{E-}2$ . In order for this good a resolution to be meaningful, the constant term  $\mathcal{C}$  has to be below this order of magnitude.

## B. Using averages

Equation 5.2 holds for the total energy  $E$  in the calorimeter. If however, one also measures the total number of particles entering the calorimeter (using a scintillator system for example, that counts minimum ionizing particles), then for each turn one can measure the average energy  $E_{av}$  of electrons. The fractional error on  $E_{av}$  does not contain a term due to the fluctuation of the number of electrons entering the calorimeter, being given by

$$\frac{\sigma_{E_{av}}^2}{\langle E_{av} \rangle^2} = \frac{\sigma_{\langle e \rangle}^2}{\langle e \rangle^2} = \frac{1}{\langle N \rangle} \left( \frac{\sigma_e^2}{\langle e \rangle^2} \right) \quad (5.14)$$

with  $\langle E_{av} \rangle = \langle e \rangle$ . For a fractional error of  $\text{PERR}$  in  $E_{av}$ , the equivalent number of electrons sampled would be given by

$$N \approx \frac{0.03153}{(\text{PERR}^2)} \quad (5.15)$$

With this method,  $PERR = .5E-2, 1.0E-2, 2.0E-2$  and  $3.0E-2$  implies 1261, 315, 79, and 35 electrons sampled, assuming no error in the measurement of  $N$ . If we sample 100,000 electrons, the fractional error in the average would be  $0.561E-3$ . For this error to be meaningful, the sampling term would have to be of this order of magnitude.

## REFERENCES

- [1] V.Bargmann, L. Michel and V.L. Telegdi, Phys. Rev. Lett. 2, 10 (1958) 435.
- [2] Particle Data Group, R.M.Barnett et al., Physical Review D54,1 (1996).
- [3] G.Barr, T.K. Gaisser and T. Stanev, Phys. Rev. D 39(1989) 3532.
- [4] MINUIT is a CERNLIB program written by F. James.
- [5] R.Assmann and J.P.Koutchouk, "Spin tune shifts due to optics imperfections", Cern SL/94-13. See also L. Arnaudon et al, "Accurate determination of the LEP beam energy by resonant depolarization ", Z.Phys.C66: 45-62,1995.
- [6] Carol Johnstone, Private Communication.
- [7] COSY INFINITY Version 7 User's guide and reference manual, M.Berz, Michigan State University Preprint MSUCL-977.
- [8] J.P.Kouthcouk, "Spin tune shift due to solenoids", CERN SL-note/93-26 (AP) (1993).
- [9] R.Rossmannith, LEP Note 525 (1985). A. Blondel, LEP note 629, (1990).

Machine	Spin tune $\nu_0$	Quadrupoles	RMS $Kl_Q$ meters <sup>-1</sup>	$\sigma_y$ meters	$\delta\nu$	$\sigma_{\delta\nu}$
46 GeV LEP	100.47	$\approx 600$	0.032	0.5E-3	5.7E-6 $\equiv 3\text{KeV}$	6.1E-5 $\equiv 30\text{KeV}$
50 GeV Muon Collider	0.5517	70	0.274	0.5E-3	-0.26E-8 $\equiv -0.24\text{KeV}$	1.66E-8 $\equiv 1.46\text{KeV}$

TABLE III. Predictions for spin tune shift  $\delta\nu$  and spread in spin tune shift  $\sigma_{\delta\nu}$  caused by quadrupoles for LEP compared to the 50 GeV muon collider ring